ACS APPLIED MATERIALS & INTERFACES

Research Article

www.acsami.org

Programmed DNAzyme-Triggered Dissolution of DNA-Based Hydrogels: Means for Controlled Release of Biocatalysts and for the Activation of Enzyme Cascades

Sivan Lilienthal, Zohar Shpilt, Fuan Wang, Ron Orbach, and Itamar Willner*

Institute of Chemistry, The Center for Nanoscience and Nanotechnology, The Hebrew University of Jerusalem, Jerusalem 91904, Israel

Supporting Information

ABSTRACT: Acrylamide/acrylamide-modified nucleic acid copolymer chains provide building units for the construction of acrylamide−DNA hydrogels. Three different hydrogels are prepared by the cross-linking of the acrylamide−DNA chains with metal ion-dependent DNAzyme sequences and their substrates. The metal ion-dependent DNAzyme sequences used in the study include the Cu^{2+}-, Mg^{2+}-, and Zn^{2+}-dependent DNAzymes. In the presence of the respective metal ions, the substrates of the respective DNAzymes are cleaved, leading to the separation of the cross-linking units and to the dissolution of the hydrogel. The different hydrogels were loaded with a fluorophore-modified dextran or with a fluorophore-functionalized glucose oxidase. Treatment of the different hydrogels with the respective ions led to the release of the loaded dextran or the enzyme, and the rates of releasing of the loaded macromolecules followed the order of $Cu^{2+} > Mg^{2+} > Zn^{2+}$. Also, the different hydrogels were loaded with the enzymes β-galactosidase (β-Gal), glucose oxidase (GOx), or horseradish peroxidase (HRP). In the presence of the appropriate metal ions, the respective hydrogels were dissolved, resulting in the activation of the β-Gal/GOx or GOx/HRP bienzyme cascades and of the β-Gal/GOx/HRP trienzyme cascade.

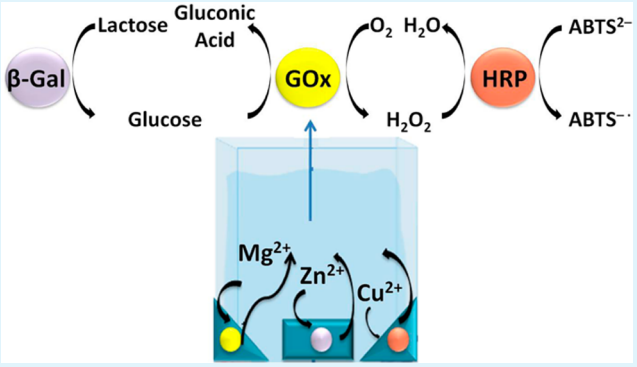

KEYWORDS: *switch, metal ion, responsive, acrylamide, polymer*

1. INTRODUCTION

Cascaded multienzyme transformations play a central role in cellular metabolism.[1,2] Ordered directional enzymatic cascades enable the efficient channeling of substrates, the stimuli-controlled branching of intracellular pathways, and the effective transport and consumption of potentially cell-toxic ingredients by localized, spatially ordered, biocatalytic sites. Two general paths, operating individually or cooperatively, lead to multienzyme cascades. One mechanism involves the organization of the enzymes on biomaterial scaffolds that allow the channeling of substrates/products along a dictated direction without diffusing into the bulk intracellular environment.[3,4] This mechanism leads to increased local concentrations of substrates/products, thus enhancing reaction rates, and may eliminate cross-talks of the reaction products with other cellular pathways.[5] Another means to control enzyme cascades involves the spatial colocalization of the biocatalysts in compartmentalized microstructures that enable the sequential operation of enzymes and their separation from other cellular components.[6,7] For example, the encapsulation of enzymes in protein cages, e.g., carboxysomes, was reported to spatially separate enzymes and allow their biocatalytic cascading.[8,9] Extensive research efforts are directed toward the development of organized nanostructures that facilitate enzyme cascades, thus mimicking the native biocatalytic pathways. Proteins, nucleic acids, and synthetic polymers were implemented as macromolecular scaffolds for cascading biocatalytic transformations.[10,11] For example, the colocalization of a two-enzyme system by protein/RNA scaffolds led to a 50-fold increase in hydrogen production in *E. coli*,[12] and a protein scaffold was applied to organize three enzymes that enhance the biosynthesis of mevalonate.[13] Also, enzymes were organized on DNA scaffolds, and the spatially ordered biocatalysts led to enhanced biocatalytic reaction rates due to the localized concentration of the reaction intermediates and their effective channeling along the biocatalytic path.[14−18] Similarly, enzymes were encapsulated within the bacteriophage P22 virus-like particles, and the kinetics of the enzyme cascade was significantly enhanced in the microcompartment.[19] Also, a three-enzyme cascade was demonstrated in an enzyme-filled synthetic polymer compartmentalized nanoreactor (polymerosome).[20−22] Besides the basic interest of programmed biocatalytic cascades in

Received: March 11, 2015
Accepted: March 31, 2015
Published: March 31, 2015

DOI: 10.1021/acsami.5b02156
ACS Appl. Mater. Interfaces 2015, 7, 8923−8931

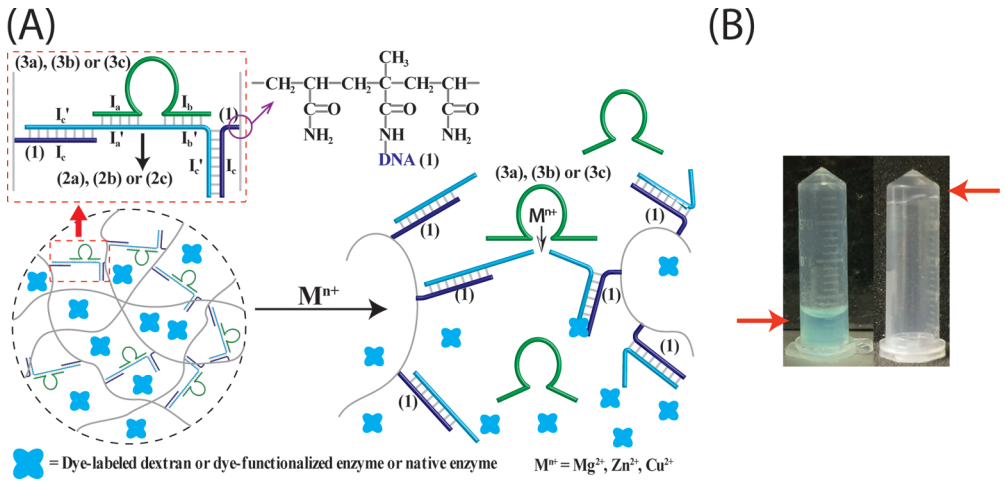

Figure 1. (A) Schematic formation of acrylamide–DNA hydrogels with entrapped dye-labeled dextran or with enzymes by the cross-linking of acrydite–nucleic acid/acrylamide copolymer chains with metal ion-dependent DNAzyme/substrate sequences and the separation of the hydrogels by the metal ion-dependent cleavage of the respective substrates. The separation of the hydrogel leads to the release of the dye-labeled dextran or the entrapped enzyme. (B) Photograph imaging the dissolution of the (**1**)/(**2c**)/(**3c**) cross-linked hydrogel upon addition of Cu^{2+} ions, 20 mM.

mimicking cellular pathways, important practical applications of enzymatic cascades may be envisaged. These include the design of biotransformations of improved efficiencies,[19] the organization of stimuli-responsive switchable biocatalytic machineries,[23] the assembly of enzyme-based logic gates,[24] and the construction of biofuel cell elements.[25,26]

Hydrogels attract substantial interest as functional matrices for the encapsulation of molecular, macromolecular, and biomolecular substrates, and the progress in the area, by addressing the different applications of loaded hydrogels, was extensively reviewed.[27−29] Among the hydrogels, nucleic acid hydrogels (DNA-based hydrogels) represent a special subclass, since the base sequences encoded in the nucleic acid units may control and dictate the hydrogel functions.[30,31] All-DNA-based hydrogels were synthesized by the cross-linking of DNA subunits using complementary base–pair duplex interactions.[32] Also, switchable all-DNA-based stimuli-responsive hydrogels were reported. For example, the cooperative ion-assisted bridging of DNA subunits led to the formation of hydrogels, and the separation of the hydrogels was stimulated by the ligand-induced elimination of the ions from the cross-linking units.[33] Copolymers of synthetic polymers, e.g., acrylamide polymers that include tethered nucleic acids, represent another broad subclass of DNA-based hydrogels. The cross-linking of the polymer chains through bridging the nucleic acid chains by duplex units or aptamer–substrate complexes was reported.[34] Stimuli-responsive switchable DNA hydrogels, undergoing reversible solution-to-hydrogel transitions, were reported.[35,36] Metal ion/ligand,[33] pH,[37,38] G-quadruplexes,[39] and photochemical stimuli[40] were applied to switch reversible hydrogel-to-solution phase transitions. Different applications of DNA-based hydrogels, and specifically stimuli-responsive hydrogels, were suggested, including controlled drug release, amplified sensing, switchable catalysis, information storage, and more.[41−43]

Catalytic nucleic acids, DNAzymes, represent synthetic sequence-specific nucleic acids mimicking the function of native enzymes.[44,45] Different catalytic nucleic acids, such as the hemin/G-quadruplex horseradish peroxidase (HRP)-mimicking DNAzyme,[46−48] metal ion-dependent hydrolytic or ligation DNAzymes,[49−54] and many other catalytic nucleic acids, were reported.[55−57] Different applications of DNAzymes were reported including their use as amplifying labels for sensing,[58−60] their use as functional units for logic gates and computing circuits,[61−66] their use as functional stimuli for the construction of various DNA machines,[67−69] and so on. The Cu^{2+} ion-dependent DNAzyme was used to cross-link acrylamide–DNA copolymer chains, and in the presence of Cu^{2+} ions, cleavage of the bridging units occurred, and the release of a hydrogel-loaded dye was reported.[70]

In the present study, we describe the assembly of DNA cross-linked acrylamide hydrogels, where the bridging units are composed of the nucleic acid sequences corresponding to metal ion-dependent DNAzymes (M^{2+} = Mg^{2+}, Zn^{2+}, Cu^{2+}).[51−53] In the presence of the respective metal ions, the selective and programmed dissolution of the respective hydrogels occurs, and the loads incorporated in the hydrogels are released. The controlled release of fluorophore-modified polymers or proteins from the hydrogels is demonstrated, and the programmed release of enzymes from the hydrogels results in the activation of enzyme cascades.

2. RESULTS AND DISCUSSION

The preparation of the functional hydrogels is depicted in Figure 1A. Copolymers consisting of acrylamide units and the acrydite–nucleic acid (**1**) units were synthesized. The nucleic acids (**3a**), (**3b**), and (**3c**) include the loop regions corresponding to the Mg^{2+}-, Zn^{2+}-, and Cu^{2+}-dependent DNAzyme sequences, respectively. These loops are extended by two arms, composed of I_a and I_b, which bind the respective domains I_a' and I_b' of the substrates of the respective DNAzymes, (**2a**), (**2b**), or (**2c**). The substrates were extended at their 3′- and 5′-ends with nucleic acid sequence I_c', that is complementary to the sequence I_c associated with (**1**). The loading of (**1**) on the copolymers was determined to be a 1:100 mole ratio (Figure S1, Supporting Information). Treatment of the hybrids (**2a**)/(**3a**), (**2b**)/(**3b**), or (**2c**)/(**3c**) with the (**1**)-copolymer chains resulted in the cross-linking of the copolymer chains to form the respective hydrogels (**1**)/(**2a**)/**3a**); (**1**)/(**2b**)/(**3b**); (**1**)/(**2c**)/(**3c**). For the detailed secondary sequence structure of the DNAzyme bridging units, see Figure S2, Supporting Information. The addition of the ions to the

DOI: 10.1021/acsami.5b02156
ACS Appl. Mater. Interfaces 2015, 7, 8923−8931

hydrogel matrices dictated the activation of the respective DNAzymes, and these cleaved the substrates (**2a**), (**2b**), or (**2c**) in the presence of Mg^{2+}, Zn^{2+}, or Cu^{2+} ions, respectively. The cleavage of the substrate units fragmented the cross-linking bridges, leading to the separation and dissolution of the hydrogels, Figure 1B.

Figure 2 depicts the rheological characterization of the different hydrogels. While the (**2a**)/(**3a**)- and the (**2b**)/(**3b**)-

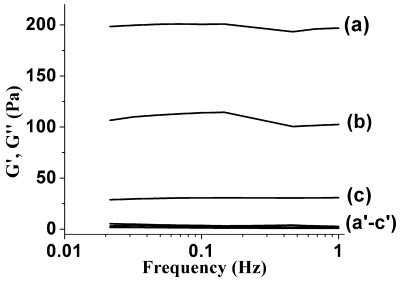

Figure 2. Rheological analysis of the different metal-dependent DNAzyme cross-linked hydrogels: Storage modules (G') of (a) the Zn^{2+}-dependent DNAzyme, (b) the Mg^{2+}-dependent DNAzyme, and (c) the Cu^{2+}-dependent DNAzyme. (a′), (b′), and (c′) correspond to the loss modules (G'') of the respective hydrogels.

cross-linked hydrogels reveal relatively high stiffness (G' = 110 and 200 Pa, respectively, and G'' = 3 and 4 Pa, respectively), the (**2c**)/(**3c**)-cross-linked hydrogel reveals lower stiffness, G' = 30 Pa and G'' = 1 Pa. The difference in the G' and G'' values for all systems implies that all matrices exist in a hydrogel state.

Fluorophore-modified proteins or polymers, e.g., tetramethylrhodamine (TMR)-functionalized dextran or Atto-590-modified glucose oxidase (GOx), were incorporated in the respective ion-sensitive DNAzyme/substrate-cross-linked acrylamide hydrogels. The resulting fluorophore-loaded hydrogels were subjected to the respective metal ions. The resulting metal ion-dependent DNAzymes stimulated the hydrolytic cleavage of the cross-linking substrate, resulting in the separation of the copolymer chains. This led to the dissolution of the hydrogels and to the release of the fluorophore-labeled macromolecules (polymers or proteins) incorporated in the hydrogels (cf. Figure 1). The time-dependent release of the TMR-functionalized dextran from the Mg^{2+} ion-dependent DNAzyme/substrate (**2a**)/(**3a**)-cross-linked hydrogel is depicted in Figure 3A, upon reacting the hydrogel with different concentrations of Mg^{2+} ions. Evidently, without Mg^{2+} ions, the release of TMR-labeled dextran is blocked, and as the concentrations of the Mg^{2+} ion increase, the release of TMR-labeled dextran is enhanced, consistent with the higher content of DNAzyme cleaving units upon increasing the concentration of Mg^{2+} ions. Also, the results indicate that the hydrogel is a stable container for the loaded TMR-labeled dextran. Similarly, the time-dependent release of TMR-labeled dextran from the Zn^{2+} ion-dependent DNAzyme/substrate (**2b**)/(**3b**)-cross-linked hydrogel, in the presence of variable concentrations of Zn^{2+} ions, is displayed in Figure 3B. As the concentration of Zn^{2+} ions is elevated, the release of TMR-labeled dextran from the hydrogel is enhanced, consistent with the higher degree of Zn^{2+} ion-dependent DNAzyme cleaving units. Similar results were observed upon incorporation of the Atto-590-modified glucose oxidase (GOx) in the (**1**)/(**2a**)/(**3a**) cross-linked hydrogel. For example, Figure 3C depicts the time-dependent fluorescence changes observed upon the Mg^{2+} ion-stimulated release of the

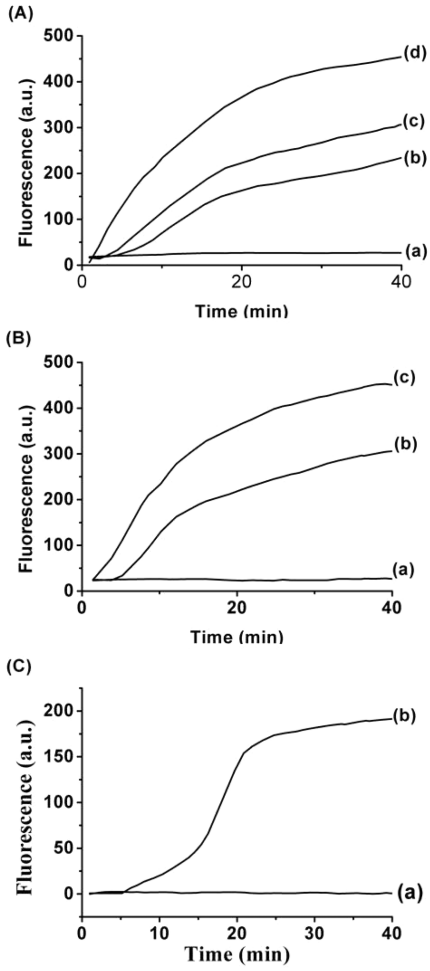

Figure 3. (A) Time-dependent release of tetramethylrhodamine (TMR)-functionalized dextran from the (**3a**)/(**2a**)-cross-linked hydrogel in the presence of different concentrations of Mg^{2+} ions: (a) 0, (b) 5, (c) 10, and (d) 20 mM. (B) Time-dependent release of TMR-functionalized dextran from the (**2b**)/(**3b**)-cross-linked hydrogel in the presence of different concentrations of Zn^{2+} ions: (a) 0, (b) 10, and (c) 20 mM. (C) Time-dependent release of GOx-Atto-590 from the (**3a**)/(**2a**)-cross-linked hydrogel in the presence of different concentrations of Mg^{2+} ions: (a) 0 and (b) 20 mM.

Atto-590-modified-GOx load from the (**1**)/(**2a**)/(**3a**) hydrogel. Similar results were obtained upon the incorporation of the Atto-590-modified GOx into the hydrogels cross-linked by the other metal ion-dependent DNAzyme/substrate bridges (see, for example, Figure S3, Supporting Information, showing the Zn^{2+} ion-stimulated release of Atto-590 functionalized GOx from the (**1**)/(**2b**)/(**3b**) hydrogel).

The release of the fluorophore-modified macromolecules from the hydrogels is selective, and treatment of the (**2a**)/(**3a**)-cross-linked hydrogel with Zn^{2+} ions or of the (**2b**)/(**3b**)-cross-linked hydrogel with Mg^{2+} ions did not lead to the release of the loaded substrates. The selective metal ion-stimulated release of fluorophore-labeled macromolecules from the different hydrogels allows then the parallel controlled release of different macromolecules from the hydrogels using the respective metal ions, Figure 4. In this experiment, the (**2b**)/(**3b**)-cross-linked, Atto-590-modified glucose oxidase (GOx)-loaded hydrogel and the (**2a**)/(**3a**)-cross-linked, TMR-dextran-loaded hydrogel were prepared. The hydrogels were loaded in a cuvette, and the controlled release of either TMR-modified dextran in the

DOI: 10.1021/acsami.5b02156
ACS Appl. Mater. Interfaces 2015, 7, 8923−8931

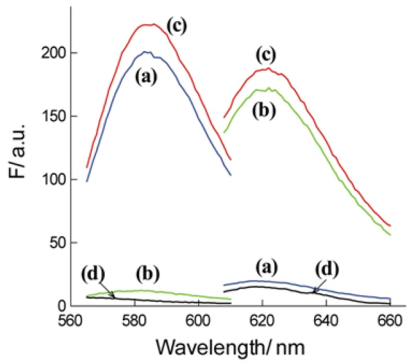

Figure 4. Parallel controlled release of different fluorophore-modified macromolecules from the hydrogels using the respective metal ions for a fixed time interval of 1 min. (a) In the presence of only Zn^{2+} ions, 20 mM. (b) In the presence of only Mg^{2+} ions, 20 mM. (c) In the presence of Mg^{2+} and Zn^{2+} ions, each 20 mM. (d) In the absence of the two metal ions. The fluorescence bands at 580 and 620 nm correspond to the TMR-dextran and Atto-590-modified GOx, respectively.

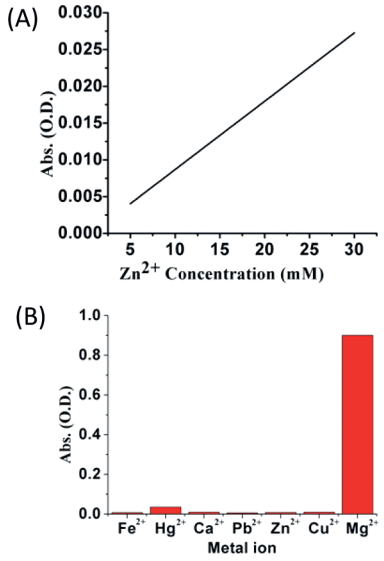

Figure 5. (A) Absorbance changes of a solution containing $ABTS^{2-}$ (50 μM) and H_2O_2 (2.2 mM) upon treatment of the 0.1 unit HRP-loaded (**2b**)/(**3c**)-cross-linked hydrogel with different Zn^{2+} concentrations. (B) Absorbance changes of a solution containing $ABTS^{2-}$ (50 μM) and H_2O_2 (2 mM) upon subjecting the HRP-loaded (**2a**)/(**3a**) hydrogel with different metal ions. The results demonstrate the selective release of HRP in the presence of Mg^{2+} ions. The concentration of metal ions in all systems is 10 mM.

presence of Zn^{2+} ions or the release of Atto-590-functionalized GOx in the presence of Mg^{2+} ions were observed, curves (a) and (b), respectively. In the presence of Mg^{2+} and Zn^{2+} ions, both hydrogels were dissociated, resulting in the release of Atto-590-GOx and TMR-dextran from the hydrogels, curve (c). A further control experiment revealed that no TMR-dextran or Atto-590-GOx were released from the hydrogels in the absence of Mg^{2+} and Zn^{2+} ions, curve (d).

The metal ion-controlled release of macromolecules was then implemented to selectively release enzymes from the hydrogels. For example, horseradish peroxidase (HRP), 0.1 units, was loaded in the (**2b**)/(**3b**) cross-linked hydrogel, and the hydrogel was separated to release HRP upon the addition of Zn^{2+} ions, 20 mM. Figure 5A depicts the activities of the released HRP using different concentrations of Zn^{2+} ions. The activity of the released HRP using different concentrations of Zn^{2+} ions was followed by the colorimetric assay that included the catalyzed oxidation of $ABTS^{2-}$ by H_2O_2 to the colored product, $ABTS^{\bullet-}$ (λ = 414 nm). As the concentration of Zn^{2+} increases, the content of the released HRP is higher, and this is reflected by the enhanced catalyzed oxidation of $ABTS^{2-}$ by H_2O_2. By applying the appropriate calibration curve relating the absorbance of $ABTS^{\bullet-}$, generated in the presence of different concentrations of HRP, we were able to estimate the number of units of HRP that were released from the hydrogel after a fixed time-interval of 15 min, in the presence of Zn^{2+} ions 20 mM. The release of the HRP was selective, and the enzyme was not released in the presence of Mg^{2+} or Cu^{2+}. The selectivity of the release of HRP from the (**1**)/(**2a**)/(**3a**) hydrogel was observed in the presence of different metal ions, such as Fe^{2+}, Pb^{2+}, Ca^{2+} and Hg^{2+}, Figure 5B. Figure S4, Supporting Information, depicts the rates of $ABTS^{\bullet-}$ formation upon releasing HRP from the different DNAzyme cross-linked hydrogels. In these experiments, all hydrogels were loaded with 0.1 U of HRP, and the release was triggered by a constant concentration of the metal ions Cu^{2+}, Mg^{2+}, and Zn^{2+}, corresponding to 20 mM. That is, the biocatalysts are most effectively released from the Cu^{2+}-dependent DNAzyme cross-linked hydrogel and most slowly released from the Zn^{2+}-dependent DNAzyme cross-linked hydrogel. The rate of the release of the enzyme from the different hydrogels is consistent with the rheology studies, Figure 2, that showed that the stiffness of the hydrogels follows the order of Zn^{2+} > Mg^{2+} > Cu^{2+} ion-dependent cross-linking DNAzyme sequences. That is, as the stiffness of the hydrogel is lower, the release of the enzyme is faster. In view of the metal ion-triggered release of enzymes from the cross-linked hydrogels, we loaded any of the hydrogels (**2a**)/(**3a**), (**2b**)/(**3b**), or (**2c**)/(**3c**) with any of the enzymes glucose oxidase (GOx), β-galactosidase (β-Gal), or horseradish peroxidase (HRP), each 0.1 units. Upon the treatment of the cross-linked hydrogels with the respective metal ions, the hydrogels were dissolved, and the enzymes were selectively released in the solution.

The availability of three different enzymes in different DNAzyme-cross-linked hydrogels and the possibility to trigger the selective release of the enzymes from the hydrogels, by the activation of the respective metal ion-dependent DNAzymes that induce the dissolution of the respective hydrogels, allowed us to design bienzyme cascades, and subsequently, trienzyme cascades. Furthermore, knowing the activities of the different biocatalysts released from the hydrogels allowed us to program the ordered sequential release of the biocatalysts, so that the most efficient cascades are designed. Figure 6 exemplifies the metal ion-activated bienzyme cascade consisting of glucose oxidase (GOx) and horseradish peroxidase (HRP). In this system, GOx is released from the (**2c**)/(**3c**)-cross-linked hydrogel using Cu^{2+} ions, and HRP is released from the (**2a**)/(**3a**)-cross-linked hydrogel using Mg^{2+} ions, Figure 6A. The GOx-mediated aerobic oxidation of glucose yields the H_2O_2 product that acts as substrate for the released HRP, that stimulates the biocatalyzed oxidation of $ABTS^{2-}$ to the colored product $ABTS^{\bullet-}$. Figure 6B shows the rate of $ABTS^{\bullet-}$ generated by the metal ion-triggered GOx/HRP biocatalytic cascade. Only in the presence of the two metal ions, Mg^{2+} and Cu^{2+}, the biocatalytic cascade is activated. Similarly, the metal ion-triggered activation of the β-Gal/GOx cascade is displayed

DOI: 10.1021/acsami.5b02156
ACS Appl. Mater. Interfaces 2015, 7, 8923−8931

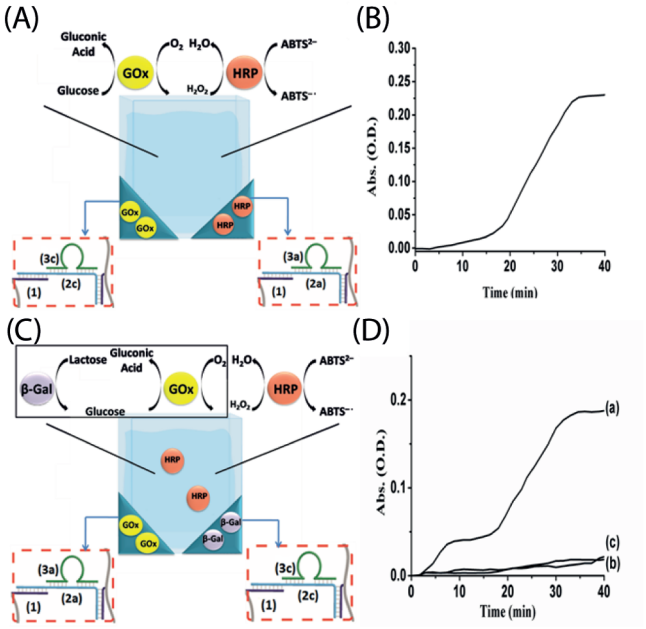

Figure 6. (A) Schematic activation of the GOx/HRP bienzyme cascade. GOx is being released from the (**1**)/(**2c**)/(**3c**) hydrogel in the presence of Cu^{2+} ions, and HRP is released from the (**1**)/(**2a**)/(**3a**) hydrogel in the presence of Mg^{2+} ions. (B) Time-dependent absorbance changes corresponding to the formation of $ABTS^{\bullet-}$ by the bienzyme cascade shown in (A). (C) Schematic activation of the β-Gal/GOx bienzyme cascade by the Cu^{2+}- and Mg^{2+}-triggered dissolution of the respective hydrogels and the release of β-Gal and GOx, respectively. The bienzyme cascade is followed by the use of HRP, as an auxiliary catalytic label in the solution. The HRP catalyzes the oxidation of $ABTS^{\bullet-}$ by the H_2O_2 formed by the bienzyme cascade, and the resulting $ABTS^{\bullet-}$ formation probes the bienzyme cascade. (D) Time-dependent absorbance changes (a) corresponding to the formation of $ABTS^{\bullet-}$ by the bienzyme cascade shown in (C) and (b and c) upon treatment of the two hydrogels with only Cu^{2+} or Mg^{2+} ions, respectively.

in Figure 6C. In this system, β-Gal is incorporated in the (**2c**)/(**3c**)-cross-linked hydrogel compartment, GOx is confined to the (**2a**)/(**3a**)-hydrogel matrix, and the solution includes lactose as a substrate. The Cu^{2+} ion-induced release of β-Gal from the (**2c**)/(**3c**) matrix leads to the hydrolysis of lactose to glucose and galactose. The resulting glucose acts as substrate for the GOx being released from the (**2a**)/(**3a**)-cross-linked hydrogel, in the presence of Mg^{2+} ions. The aerobic oxidation of glucose by GOx yields H_2O_2 as the product of the bienzyme cascade. The addition of HRP and $ABTS^{2-}$ to the solution provides an auxiliary biocatalytic probe to assay the β-Gal/GOx cascade through the H_2O_2-catalyzed oxidation of $ABTS^{2-}$ to $ABTS^{\bullet-}$. Control experiments revealed that no $ABTS^{\bullet-}$ was formed upon the treatment of the system with Cu^{2+} ions or Mg^{2+} ions only. These results imply that the dissociation of both hydrogels is crucial to activate the β-Gal/GOx cascade that yields the product H_2O_2 being analyzed by the auxiliary HRP probe. The related activation of the GOx/HRP cascade and of the β-Gal/GOx cascade were explored using other metal ion-dependent DNAzymes matrices. For example, Figure S5, Supporting Information, depicts the activation of the GOx/HRP cascade by Mg^{2+} and Zn^{2+} ions in the system consisting of the GOx-loaded (**1**)/(**2a**)/(**3a**) and the HRP-loaded (**1**)/(**2b**)/(**3b**) hydrogels. Similarly, Figure S6, Supporting Information, exemplifies the selective activation of the β-Gal/GOx cascade using the combination of two metal ion-dependent DNAzyme hydrogels, where the β-Gal was loaded in the (**1**)/(**2a**)/(**3a**) hydrogel, GOx was entrapped in the (**1**)/(**2b**)/(**3b**) hydrogel, the two enzymes were released by the addition of Mg^{2+} and Zn^{2+} ions, respectively. From Figure 6B,D (and also Figures S5 and S6, Supporting Information), one might realize that the activation of the bienzyme cascades involves and initial inefficient formation of the biocatalyzed reaction product (or, eventually, the formation of a steady-state low concentration of the product, e.g., Figure 6D), followed by a rapid effective formation of the product of the biocatalytic cascade. The initial inefficient formation of the product is attributed to the primary partial decomposition of the hydrogels by the DNAzymes and the association of the enzymes to the hydrogel interface. The digestion of the hydrogel with time dissociates the associated enzyme, resulting in the rapid formation of the product of the bienzyme cascades.

In the next step, we examined the activation of the three-enzyme cascade stimulated by the dissolution of three different hydrogels by the respective metal ions. Specifically, we wanted to examine the effect of the rate of dissolution of the different metal-dependent hydrogels on the observed rate of the three-enzyme cascade, Figure 7A. Toward this end, we incorporated

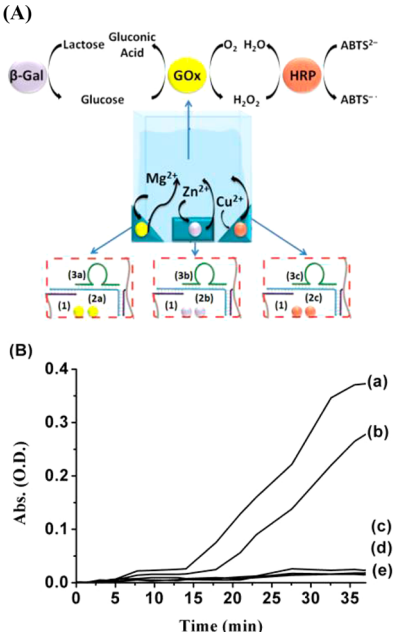

Figure 7. (A) Schematic operation of the three-enzyme cascade β-Gal/GOx/HRP by the ion-stimulated release of the enzymes from the respective hydrogels. In the specific example, the β-Gal is released from the Zn^{2+}-dependent DNAzyme-bridged hydrogel, GOx is released from the Mg^{2+}-dependent DNAzyme-bridged hydrogel, and HRP is released from the Cu^{2+}-dependent DNAzyme-bridged hydrogel. (B) Time-dependent absorbance changes resulting upon the activation of the trienzyme cascade: (a) Upon releasing the β-Gal from the Cu^{2+}-dependent DNAzyme-bridged hydrogel, (**1**)/(**2c**)/(**3c**), GOx from the Mg^{2+}-dependent DNAzyme-bridged hydrogel (**1**)/(**2a**)/(**3a**), and HRP from the Zn^{2+}-dependent DNAzyme-bridged hydrogel (**1**)/(**2b**)/(**3b**); (b) upon releasing β-Gal from the (**1**)/(**2b**)/(**3b**) hydrogel, GOx from (**1**)/(**2a**)/(**3a**) hydrogel, and HRP from the (**1**)/(**2c**)/(**3c**) hydrogel, as schematically presented in (A); (c–e) showing the absorbance changes of the three hydrogel systems shown in (A) in the presence of Cu^{2+}/ Zn^{2+}, Mg^{2+}/ Zn^{2+}, or Cu^{2+}/ Mg^{2+}, respectively.

DOI: 10.1021/acsami.5b02156
ACS Appl. Mater. Interfaces 2015, 7, 8923–8931

into each of the hydrogels 0.1 units of any of the biocatalysts. This low content of enzyme was used in order to observe experimentally the relationships between the rates of dissociation of the hydrogels and the overall reaction of the three-enzyme cascade. In the first system in this comparison, the β-Gal was incorporated in the Cu^{2+}-dependent DNAzyme cross-linked hydrogel (**2c**)/(**3c**) (fastest hydrogel dissolution), GOx was loaded in the Mg^{2+}-dependent DNAzyme cross-linked hydrogel (**2a**)/(**3a**) (medium rate dissolution of hydrogel), and HRP was immobilized in the Zn^{2+}-dependent DNAzyme-cross-linked hydrogel, (**2b**)/(**3b**) (the slowest rate of dissolution of the hydrogel). Figure 7B, curve (a), depicts the rate of $ABTS^{\bullet-}$ formation as a result of the activation of the three-enzyme cascade, upon dissolving the respective hydrogel by the simultaneous addition of Cu^{2+}, Mg^{2+}, and Zn^{2+} to the hydrogel mixture. For comparison, Figure 7B, curve (b), shows the activation of the three-enzyme cascade from a system that includes β-Gal loaded in the (**2b**)/(**3b**) hydrogel (lowest release rate) and HRP was immobilized in the (**2c**)/(**3c**) hydrogel (highest release rate). One may realize that the rate of $ABTS^{\bullet-}$ formation is ca. 1.5-fold lower than in the previous system. These results suggest that the rate of the enzyme cascade is controlled by the relative rates of release of the biocatalysts from the respective hydrogels and the availability of the respective substrates to activate the enzyme cascade. That is, in the first system, the β-Gal-catalyzed hydrolysis of lactose to yield glucose and the subsequent aerobic oxidation of glucose, in the presence of GOx, yield a pool of the H_2O_2 substrate that can be utilized by the slowly released HRP. In turn, in the second system, the inefficient release of β-Gal by the (**2b**)/(**3b**) hydrogel leads to an inefficient oxidation of glucose by GOx and to a poor reservoir of the resulting H_2O_2. Thus, despite the effective release of HRP from the (**2c**)/(**3c**)-cross-linked hydrogel in the presence of Cu^{2+} ions, the rate of oxidation of $ABTS^{2-}$ by H_2O_2 is lower.

Previous studies have demonstrated that the spatial organization of two communicating enzymes by means of a DNA scaffold enhances the bienzyme cascade by the localized concentration of the substrates/products at the biocatalytic sites.[9] The local concentration of the product generated by one enzyme in the vicinity of the second enzyme, where the product of the first enzyme acts as substrate for the second enzyme, overcomes diffusion barriers of the reaction substrate and then enhances the biocatalytic cascade. Accordingly, the enzymes GOx and HRP were modified with the complementary nucleic acids (**4**) and (**5**), respectively. The (**4**)-modified GOx (0.04 units) and the (**5**)-modified HRP (0.04 units) were loaded in the Mg^{2+}-dependent DNAzyme cross-linked hydrogel (**2a**)/(**3a**) and in the Zn^{2+}-dependent DNAzyme cross-linked hydrogel, (**2b**)/(**3b**), respectively. Note that the loading of the nucleic acid-functionalized biocatalysts is 2.5-fold lower than the loading of the enzymes in the previous experiments. The two hydrogels were subjected to Zn^{2+} and Mg^{2+} ions, resulting in the dissociation of the respective hydrogels and the release of the (**4**)-GOx and (**5**)-HRP into the aqueous phase, Figure 8A. Note that the dissolution of the hydrogels occurred on a time-scale of 10−30 min. The release of the nucleic acid-modified GOx and HRP then allowed the activation of the bienzyme cascade. Figure 8B, curve (a), shows the time-dependent absorbance changes upon activation of the bienzyme cascade by the (**4**)-GOx/(**5**)-HRP conjugate. For comparison, Figure 8B, curve (b), depicts the time-dependent absorbance changes stimulated by the bienzyme cascade, upon releasing

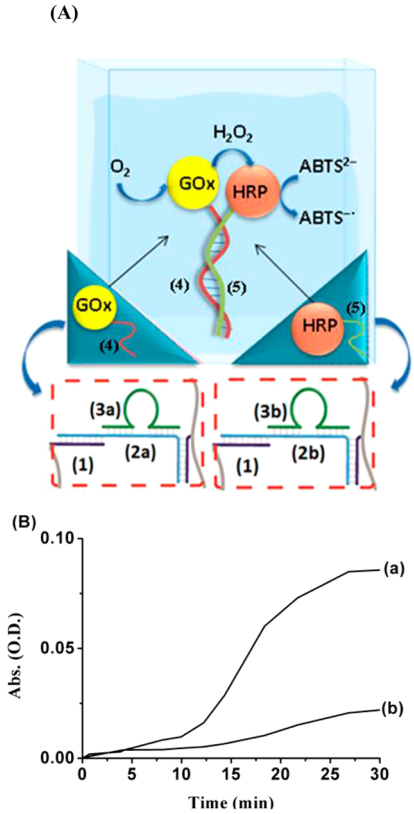

Figure 8. (A) Schematic activation of a bienzyme catalytic cascade by the assembly of GOx and HRP on a duplex DNA scaffold of complementary nucleic acids functionalizing the two enzymes. (B) Time-dependent absorbance changes of $ABTS^{\bullet-}$ upon: (a) Activation of the bienzyme cascade shown in (A). (b) The enzyme cascade activated by GOx and HRP released from the hydrogels. In both systems, the (**1**)/(**2a**)/(**3a**) and the (**1**)/(**2b**)/(**3b**) hydrogels are loaded with 0.04 U of the nucleic acid, (**4**)-functionalized GOx, and the nucleic acid, (**5**)-modified HRP, respectively, or with 0.04 U of the nonmodified GOx and HRP, respectively. The release of the enzyme from the hydrogels is triggered by Mg^{2+} and Zn^{2+}, respectively. In all systems, the solution includes $ABTS^{2-}$ (50 μM) and H_2O_2 (2.2 mM).

from the respective hydrogels the same amounts of the enzymes that are not modified by the nucleic acids (**4**) and (**5**). Evidently, minute absorbance changes are observed, implying that the bienzyme cascade is inefficient. The inefficient biocatalytic cascade stimulated by the nonmodified enzymes GOx and HRP is attributed to the low concentrations of the biocatalysts introduced into the solution upon dissociation of the two hydrogels. The random distributions of the enzymes lead to low bulk concentrations of H_2O_2 and to the diffusion-controlled, inefficient, communication between the enzymes. In turn, the duplex formation between the (**4**)-GOx and (**5**)-HRP leads to the spatial organization of the two biocatalysts in close proximity. In this supramolecular structure, the H_2O_2 formed by GOx yields a high local concentration at the HRP interface, leading to the effective rapid oxidation of $ABTS^{2-}$.

3. CONCLUSION

The present study has introduced a versatile method to assemble DNA-based acrylamide hydrogels by cross-linking the acrylamide chains with metal-dependent DNAzyme sequences that were hybridized with their substrates. In the presence of the respective ions (M^{2+} = Zn^{2+}, Mg^{2+}, or Cu^{2+}), the bridging

DOI: 10.1021/acsami.5b02156
ACS Appl. Mater. Interfaces 2015, 7, 8923−8931

Table 1. DNA Sequences That Were Used in This Study

no.	sequence
1	TTTTCTTCATTGTTT
2a	AAACAATGAAGATCCCAAACT TrAG GAAAGCCCAAAACAATGAAGA
2b	AAACAATGAAGAAAACCGACTAGACGTTGAAGGATACCAGGGAAACAATGAAGAAAA
2c	AAACAATGAAGAAAAGCTTCTTTCTAATACGGCTTACCTAAACAATGAAGAAAA
3a	TTGGGCTTTCAGCGATTAAGGACCTTACACCCATGTAGTTTGGGAT
3b	CCCTGGTATCTAGTTGAGCTGTCTAGTCGG
3c	GGTAAGCCTGGGCCTCTTTCTTTTTAAGAAAGAAC
4	*SH-CGAAGAAGAGAAGCTAGTCAACCTGTCCTATCTATGATGG*
5	CCATCATAGATAGGACAGGTTGACTAGCTTCTCTTCTCGA-SH

units were cleaved by the respective metal-dependent DNAzymes leading to the selective dissociation of the different hydrogels. Three different enzymes (β-Gal, GOx, HRP) were immobilized in the sequence-specific DNAzyme-bridged hydrogels, and the metal ion-triggered dissociation and release of the enzymes was demonstrated. By using mixtures of DNAzyme-bridged hydrogels that incorporated two different enzymes, bienzyme cascades were activated by the ion-triggered dissociation of the hydrogels and the release of the two enzymes. Similarly, by incorporating three enzymes (β-Gal, GOx, HRP) in three different DNAzyme-cross-linked hydrogel matrices, the programmed three enzyme cascade β-Gal/GOx/HRP was activated by the metal ion-triggered dissociation of the hydrogels. We find that the effectiveness of the enzyme cascade is controlled by the rate of the ion-triggered dissociation of the hydrogels. The availability of many different ion-dependent DNAzymes and even other cofactor-dependent hydrolytic cleavage DNAzymes (e.g., the histidine-dependent DNAzyme)[55] suggests that a rich library of stimuli-triggered hydrogels may be assembled. Such systems could lead to complex multibiocatalytic cascades or branched biocatalytic pathways.

A further interesting result of the study includes the use of nucleic acid-modified enzymes as a hybrid system for the promotion of a biocatalytic cascade, under conditions where the unmodified enzymes poorly communicate. In this system, the hybridization between the nucleic acid tethers modifying the biocatalysts leads to spatial proximity between the communicating enzymes, allowing the funneling of the locally concentrated product generated by one enzyme to act as substrate for the second biocatalyst, thus eliminating diffusion barriers. The possibilities to self-assemble nucleic acid nanostructures suggest that multienzyme cascades of enhanced complexities could be organized on such structures. Furthermore, the triggered dissolution of the hydrogels by means of DNAzyme-stimulated cleavage of the nucleic acid bridges yields fragmented nucleic acids. At this stage, these oligonucleotides act as "waste" products. Nonetheless, one might envisage the use of these nucleic acids as activators of catalytic cascades (e.g., the hybridization chain reaction),[39] thus allowing the evolution of complex nucleic acid catalytic circuitries.[34a]

4. EXPERIMENTAL SECTION

Materials. Horseradish peroxidase (HRP), glucose oxidase (GOx), β-galactosidase (β-Gal), sodium nitrate, zinc chloride, magnesium chloride, copper nitrate, HEPES sodium salt, HEPES, lactose, glucose, 2,2′-azino-bis(3-ethylbenzothiazoline-6-sulfonic acid) diammonium salt (ABTS), hydrogen peroxide solution (3%), ammonium persulfate (APS), *N*,*N*,*N*′,*N*′-tetramethylethylenediamine (TEMED), Atto 590 NHS ester, tetramethylrhodamine (TMR)-functionalized dextran, and acrylamide solution (40%) were purchased from Sigma–Aldrich. All oligonucleotides including (**1**)-acridite were purchased from Integrated DNA Technologies Inc. (Coralville, IA). Table 1 shows the sequences of the oligonucleotides used in the study. The oligonucleotides were dissolved in distilled water (pH = 7) to yield stock solutions of 100 μM.

Synthesis of the Acrylamide/Acrylamide Nucleic Acid Copolymer, Preparation of the Loaded Hydrogels, the Metal Ion-Stimulated Dissolution of the Hydrogels and the Release of the Loads. *Preparation of the (1)-Modified Copolymer.* An aqueous mixture of 10 μL of 40% acrylamide with 200 μL of the (**1**)-acrydite (100 μM) was prepared, and nitrogen was bubbled through the solution. Subsequently, 8 μL of a 0.1 mL aqueous solution that contained 1 mg of APS and 5 μL of TEMED in 95 μL of water were added to the mixture of the monomers to induce polymerization. The resulting mixture was allowed to react at room temperature for 5 min and subsequently at 4 °C for an additional time interval of 10 h. The concentration of the resulting copolymer and the acrylamide–DNA molar ratio in the copolymer were determined spectroscopically.

Preparation of the Loaded Acrylamide/Acrylamide–DNA Cross-Linked Hydrogels. To the (**1**)-functionalized copolymer, 0.3 M, in water, 40 μL, 10 μL of a HEPES buffer solution (0.2 M), that included 5 M sodium nitrate, was added. The respective enzyme, 0.1 units, in 5 μL of HEPES buffer were added to the mixture. To this mixture, 20 μL of the DNA strands (**2a**), (**2b**), or (**2c**) (100 μM) were added, and 20 μL of a 100 μM solution of (**3a**), (**3b**), or (**3c**) were added. The mixture was allowed to interact at room temperature for a time interval of 30 min to yield the respective hydrogel.

Dissolution of the Hydrogels and the Release of the Enzyme Loads. The resulting enzyme-loaded hydrogel, 95 μL, was introduced into a quartz cuvette rinsed with 400 μL of HEPES buffer solution, and 2 mL of the HEPES buffer solution was introduced into the cuvette. The respective metal ions, at the appropriate concentration, were added to the solution. The time-dependent dissolution of the hydrogels and the amounts of the released enzymes were probed by assaying the activity of the released enzymes.

Determination of the Ratio of Acrylamide/Acrydite-Nucleic Acid Units in Copolymer Chains. To a solution containing acrylamide polymer, variable concentrations of the respective acrydite nucleic acids, 0.1, 0.2, 0.3, 0.4, 0.5, 0.6, 0.7, and 0.8 μM, were added, and the absorption spectra of the different solutions were recorded. The increase in the absorbance at λ = 200 nm corresponded to the nonsubstituted polyacrylamide chains, while the absorbance at λ = 260 nm corresponded to the acrydite–nucleic acid units. An appropriate calibration curve corresponding to the molar ratio of the nucleic acids in the copolymer and the acrylamide monomer units was derived. On the basis of this calibration curve, the ratio of acrydite-nucleic acid/acrylamide in the different copolymers was evaluated spectroscopically (see Figure S1, Supporting Information).

■ ASSOCIATED CONTENT

Supporting Information

The secondary structure of the different DNAzymes, spectroscopic characterization of the acrylamide/acrydite nucleic acid copolymer, and spectroscopic characterization of

DOI: 10.1021/acsami.5b02156
ACS Appl. Mater. Interfaces 2015, 7, 8923–8931

the release of enzymes from the hydrogels. This material is available free of charge via the Internet at http://pubs.acs.org.

AUTHOR INFORMATION

Corresponding Author

*E-mail: willnea@vms.huji.ac.il.

Author Contributions

The manuscript was written through contributions of all authors. All authors have given approval to the final version of the manuscript.

Notes

The authors declare no competing financial interest.

ACKNOWLEDGMENTS

This research is supported by the EU FET Open MICRE-Agents Project #318671.

REFERENCES

(1) Miles, E. W.; Rhee, S.; Davies, D. R. The Molecular Basis of Substrate Channeling. *J. Biol. Chem.* **1999**, *274*, 12193−12196.

(2) Martin, W. Evolutionary Origins of Metabolic Compartmentalization in Eukaryotes. *Philos. Trans. R. Soc., B* **2010**, *365*, 847−855.

(3) Conrado, R. J.; Varner, J. D.; DeLisa, M. P. Engineering the Spatial Organization of Metabolic Enzymes: Mimicking Nature's Synergy. *Curr. Opin. Biotechnol.* **2008**, *19*, 492−499.

(4) Chen, A. H.; Silver, P. A. Designing Biological Compartmentalization. *Trends Cell Biol.* **2012**, *22*, 662−670.

(5) Agapakis, C. M.; Boyle, P. M.; Silver, P. A. Natural Strategies for the Spatial Optimization of Metabolism in Synthetic Biology. *Nat. Chem. Biol.* **2012**, *8*, 527−535.

(6) Tanaka, S.; Sawaya, M. R.; Yeates, T. O. Structure and Mechanisms of a Protein-Based Organelle in *Escherichia coli*. *Science* **2010**, *327*, 81−84.

(7) Sutter, M.; Boehringer, D.; Gutmann, S.; Guenther, S.; Prangishvili, D.; Losserner, M. J.; Stetter, K. O.; Weber-Ban, E.; Ban, N. Structural Basis of Enzyme Encapsulation into a Bacterial Nanocompartment. *Nat. Struct. Mol. Biol.* **2008**, *15*, 939−947.

(8) Marguet, M.; Bonduelle, C.; Lecommandoux, S. Multicompartmentalized Polymeric Systems: Towards Biomimetic Cellular Structure and Function. *Chem. Soc. Rev.* **2013**, *42*, 512−529.

(9) Bolinger, P.; Stamou, D.; Vogel, H. An Integrated Self-Assembled Nanofluidic System for Controlled Biological Chemistries. *Angew. Chem., Int. Ed.* **2008**, *47*, 5544−5549.

(10) Renggli, K.; Baumann, P.; Langowska, K.; Onaca, O.; Bruns, N.; Meier, W. Selective and Responsive Nanoreactors. *Adv. Funct. Mater.* **2011**, *21*, 1241−1259.

(11) Uchida, M.; Klem, M. T.; Allen, M.; Suci, P.; Flenniken, M.; Gillitzer, E.; Varpness, Z.; Liepold, L. O.; Young, M.; Douglas, T. Biological Containers: Protein Cages as Multifunctional Nanoplatforms. *Adv. Mater.* **2007**, *19*, 1025−1042.

(12) Delebecque, C. J.; Lindner, A. B.; Silver, P. A.; Aldaye, F. A. Organization of Intracellular Reactions with Rationally Designed RNA Assemblies. *Science* **2011**, *333*, 470−474.

(13) Dueber, J. E.; Wu, G. C.; Malmirchegini, G. R.; Moon, T. S.; Petzold, C. J.; Ullal, A. V.; Prather, K. L.; Keasling, J. D. Synthetic Protein Scaffolds Provide Modular Control Over Metabolic Flux. *Nat. Biotechnol.* **2009**, *27*, 753−759.

(14) Wilner, O. I.; Shimron, S.; Weizmann, Y.; Wang, Z. G.; Willner, I. Self-Assembly of Enzymes on DNA Scaffolds: En Route to Biocatalytic Cascades and the Synthesis of Metallic Nanowires. *Nano Lett.* **2009**, *9*, 2040−2043.

(15) Wilner, O. I.; Weizmann, Y.; Gill, R.; Lioubashevski, O.; Freeman, R.; Willner, I. Enzyme Cascades Activated on Topologically Programmed DNA Scaffolds. *Nat. Nanotechnol.* **2009**, *4*, 249−254.

(16) Fu, J. L.; Liu, M. H.; Liu, Y.; Woodbury, N. W.; Yan, H. Interenzyme Substrate Diffusion for an Enzyme Cascade Organized on Spatially Addressable DNA Nanostructures. *J. Am. Chem. Soc.* **2012**, *134*, 5516−5519.

(17) Fu, J.; Liu, M.; Liu, Y.; Yan, H. Spatially-Interactive Biomolecular Networks Organized by Nucleic Acid Nanostructures. *Acc. Chem. Res.* **2012**, *45*, 1215−1226.

(18) Schoffelen, S.; van Hest, J. C. M. Multi-Enzyme Systems: Bringing Enzymes Together in Vitro. *Soft Matter* **2012**, *8*, 1736−1746.

(19) Patterson, D. P.; Schwarz, B.; Waters, R. S.; Gedeon, T.; Douglas, T. Encapsulation of an Enzyme Cascade within the Bacteriophage P22 Virus-Like Particle. *ACS Chem. Biol.* **2014**, *9*, 359−365.

(20) Peters, R. J.; Marguet, M.; Marais, S.; Fraaije, M. W.; van Hest, J. C.; Lecommandoux, S. Cascade Reactions in Multicompartmentalized Polymersomes. *Angew. Chem., Int. Ed.* **2014**, *53*, 146−150.

(21) Gaitzsch, J.; Appelhans, D.; Wang, L.; Battaglia, G.; Voit, B. Synthetic Bio-Nanoreactor: Mechanical and Chemical Control of Polymersome Membrane Permeability. *Angew. Chem., Int. Ed.* **2012**, *51*, 4448−4451.

(22) Nardin, C.; Thoeni, S.; Widmer, J.; Winterhalter, M.; Meier, W. Nanoreactors Based on (Polymerized) ABA-Triblock Copolymer Vesicles. *Chem. Commun.* **2000**, *15*, 1433−1434.

(23) Liu, M.; Fu, J.; Hejesen, C.; Yang, Y.; Woodbury, N. W.; Gothelf, K.; Liu, Y.; Yan, H. A DNA Tweezer-Actuated Enzyme Nanoreactor. *Nat. Commun.* **2013**, *4*, 2127.

(24) Niazov, T.; Baron, R.; Katz, E.; Lioubashevski, O.; Willner, I. Concatenated Logic Gates Using Four Coupled Biocatalysts Operating in Series. *Proc. Natl. Acad. Sci. U.S.A.* **2006**, *103*, 17160−17163.

(25) Xu, S.; Minteer, S. D. Investigating the Impact of Multi-Heme Pyrroloquinoline Quinone-Aldehyde Dehydrogenase Orientation on Direct Bioelectrocatalysis via Site Specific Enzyme Immobilization. *ACS Catal.* **2013**, *3*, 1756−1763.

(26) Hickey, D. P.; Giroud, F.; Schmidtke, D. W.; Glatzhofer, D. T.; Minteer, S. D. Enzyme Cascade for Catalyzing Sucrose Oxidation in a Biofuel Cell. *ACS Catal.* **2013**, *3*, 2729−2737.

(27) Kopecek, J.; Yang, J. Smart Self-Assembled Hybrid Hydrogel Biomaterials. *Angew. Chem., Int. Ed.* **2012**, *51*, 7396−7417.

(28) Lee, K. Y.; Mooney, D. J. Hydrogels for Tissue Engineering. *Chem. Rev.* **2001**, *101*, 1869−1879.

(29) Peppas, N. A.; Hilt, J. Z.; Khademhosseini, A.; Langer, R. Hydrogels in Biology and Medicine: From Molecular Principles to Bionanotechnology. *Adv. Mater.* **2006**, *18*, 1345−1360.

(30) Roh, Y. H.; Ruiz, R. C.; Peng, S.; Lee, J. B.; Luo, D. Engineering DNA-Based Functional Materials. *Chem. Soc. Rev.* **2011**, *40*, 5730−5744.

(31) Liu, J. Oligonucleotide-Functionalized Hydrogels as Stimuli Responsive Materials and Biosensors. *Soft Matter* **2011**, *7*, 6757−6767.

(32) Um, S. H.; Lee, J. B.; Park, N.; Kwon, S. Y.; Umbach, C. C.; Luo, D. Enzyme-Catalysed Assembly of DNA Hydrogel. *Nat. Mater.* **2006**, *5*, 797−801.

(33) Guo, W.; Qi, X. J.; Orbach, R.; Lu, C. H.; Freage, L.; Mironi-Harpaz, I.; Seliktar, D.; Yang, H. H.; Willner, I. Reversible Ag^{+}-Crosslinked DNA Hydrogels. *Chem. Commun.* **2014**, *50*, 4065−4068.

(34) Liedl, T.; Dietz, H.; Yurke, B.; Simmel, F. Controlled Trapping and Release of Quantum Dots in a DNA-Switchable Hydrogel. *Small* **2007**, *3*, 1688−1693.

(35) Xing, Y.; Cheng, E.; Yang, Y.; Chen, P.; Zhang, T.; Sun, Y.; Yang, Z.; Liu, D. Self-Assembled DNA Hydrogels with Designable Thermal and Enzymatic Responsiveness. *Adv. Mater.* **2011**, *23*, 1117−1121.

(36) Dave, N.; Chan, M. Y.; Huang, P. J.; Smith, B. D.; Liu, J. Regenerable DNA-Functionalized Hydrogels for Ultrasensitive, Instrument-Free Mercury(II) Detection and Removal in Water. *J. Am. Chem. Soc.* **2010**, *132*, 12668−12673.

(37) Cheng, E.; Xing, Y.; Chen, P.; Yang, Y.; Sun, Y.; Zhou, D.; Xu, L.; Fan, Q.; Liu, D. A pH-Triggered, Fast-Responding DNA Hydrogel. *Angew. Chem., Int. Ed.* **2009**, *48*, 7660−7663.

(38) Guo, W.; Lu, C. H.; Qi, X. J.; Orbach, R.; Fadeev, M.; Yang, H. H.; Willner, I. Switchable Bifunctional Stimuli-Triggered Poly-*N*-

DOI: 10.1021/acsami.5b02156
ACS Appl. Mater. Interfaces 2015, 7, 8923−8931

isopropylacrylamide/DNA Hydrogels. *Angew. Chem., Int. Ed.* **2014**, *53*, 10134−10138.
(39) Lu, C. H.; Qi, X. J.; Orbach, R.; Yang; Mironi-Harpaz, I.; Seliktar, D.; Willner, I. Switchable Catalytic Acrylamide Hydrogels Cross-Linked by Hemin/G-Quadruplexes. *Nano Lett.* **2013**, *13*, 1298−1302.
(40) Kang, H.; Liu, H.; Zhang, X.; Yan, J.; Zhu, Z.; Peng, L.; Yang, H.; Kim, Y.; Tan, W. Photoresponsive DNA-Cross-Linked Hydrogels for Controllable Release and Cancer Therapy. *Langmuir* **2011**, *27*, 399−408.
(41) Joseph, K. A.; Dave, N.; Liu, J. Electrostatically Directed Visual Fluorescence Response of DNA-Functionalized Monolithic Hydrogels for Highly Sensitive Hg^{2+} Detection. *ACS Appl. Mater. Interfaces* **2011**, *3*, 733−739.
(42) Guo, W.; Lu, C. H.; Orbach, R.; Wang, F.; Oi, X. J.; Cocconello, A.; Seliktar, D.; Willner, I. pH-Stimulated DNA Hydrogels Exhibiting Shape-Memory Properties. *Adv. Mater.* **2015**, *27*, 73−78.
(43) Lee, J. B.; Peng, S.; Yang, D.; Roh, Y. H.; Funabashi, H.; Park, N.; Rice, E. J.; Chen, L.; Long, R.; Wu, M.; Luo, D. A Mechanical Metamaterial Made from a DNA Hydrogel. *Nat. Nanotechnol.* **2012**, *7*, 816−820.
(44) Breaker, R. R. DNA Enzymes. *Nat. Biotechnol.* **1997**, *15*, 427−431.
(45) Silverman, S. K. Deoxyribozymes: DNA Catalysts for Bioorganic Chemistry. *Org. Biomol. Chem.* **2004**, *2*, 2701−2706.
(46) Travascio, P.; Li, Y.; Sen, D. DNA-Enhanced Peroxidase Activity of a DNA-Aptamer-Hemin Complex. *Chem. Biol.* **1998**, *5*, 505−517.
(47) Nakayama, S.; Sintim, H. O. Colorimetric Split G-Quadruplex Probes for Nucleic Acid Sensing: Improving Reconstituted DNAzyme's Catalytic Efficiency via Probe Remodeling. *J. Am. Chem. Soc.* **2009**, *131*, 10320−10333.
(48) Golub, E.; Freeman, R.; Willner, I. A Hemin/G-Quadruplex Acts as an NADH Oxidase and NADH Peroxidase Mimicking DNAzyme. *Angew. Chem., Int. Ed.* **2011**, *50*, 11710−11714.
(49) Cuenoud, B.; Szostak, J. W. A DNA Metalloenzyme with DNA Ligase Activity. *Nature* **1995**, *375*, 611−614.
(50) Chapman, K. B.; Szostak, J. W. Isolation of a Ribozyme with 5′-5′ Ligase Activity. *Chem. Biol.* **1995**, *2*, 325−333.
(51) Breaker, R. R.; Joyce, G. F. A DNA Enzyme with Mg^{2+}-Dependent RNA Phosphoesterase Activity. *Chem. Biol.* **1995**, 655−660.
(52) Liu, J.; Lu, Y. A DNAzyme Catalytic Beacon Sensor for Paramagnetic Cu^{2+} Ions in Aqueous Solution with High Sensitivity and Selectivity. *J. Am. Chem. Soc.* **2007**, *129*, 9838−9839.
(53) Gu, H.; Furukawa, K.; Weinberg, Z.; Berenson, D. F.; Breaker, R. R. Small, Highly Active DNAs That Hydrolyze DNA. *J. Am. Chem. Soc.* **2013**, *135*, 9121−9129.
(54) Travascio, P.; Witting, P. K.; Mauk, A. G.; Sen, D. The Peroxidase Activity of a Hemin−DNA Oligonucleotide Complex: Free Radical Damage to Specific Guanine Bases of the DNA. *J. Am. Chem. Soc.* **2001**, *123*, 1337−1348.
(55) Roth, A.; Breaker, R. R. An Amino Acid as a Cofactor for a Catalytic Polynucleotide. *Proc. Natl. Acad. Sci. U.S.A.* **1998**, *95*, 6027−6031.
(56) Breaker, R. R.; Joyce, G. F. A DNA Enzyme that Cleaves RNA. *Chem. Biol.* **1994**, *1*, 223−229.
(57) Brown, A. K.; Liu, J.; He, Y.; Lu, Y. Biochemical Characterization of a Uranyl Ion-Specific DNAzyme. *ChemBioChem* **2009**, *10*, 486−492.
(58) Liu, J.; Cao, Z.; Lu, Y. Functional Nucleic Acid Sensors. *Chem. Rev.* **2009**, *109*, 1948−1998.
(59) Gerasimova, Y. V.; Kolpashchikov, D. M. Nucleic Acid Detection Using MNAzymes. *Chem. Biol.* **2010**, *17*, 104−106.
(60) Wang, F.; Lu, C. H.; Willner, I. From Cascaded Catalytic Nucleic Acids to Enzyme-DNA Nanostructures: Controlling Reactivity, Sensing, Logic Operations, and Assembly of Complex Structures. *Chem. Rev.* **2014**, *114*, 2881.
(61) Orbach, R.; Willner, B.; Willner, I. Catalytic Nucleic Acids (DNAzymes) as Functional Units for Logic Gates and Computing Circuits: From Basic Principles to Practical Applications. *Chem. Commun.* **2015**, *51*, 4144−4160.
(62) Elbaz, J.; Lioubashevski, O.; Wang, F.; Remacle, F.; Levine, R. D.; Willner, I. DNA Computing Circuits Using Libraries of DNAzyme Subunits. *Nat. Nanotechnol.* **2010**, *5*, 417−422.
(63) Elbaz, J.; Wang, F.; Remacle, F.; Willner, I. pH-Programmable DNA Logic Arrays Powered by Modular DNAzyme Libraries. *Nano Lett.* **2012**, *12*, 6049−6054.
(64) Zhu, J.; Zhang, L.; Li, T.; Dong, S.; Wang, E. Enzyme-Free Unlabeled DNA Logic Circuits Based on Toehold-Mediated Strand Displacement and Split G-Quadruplex Enhanced Fluorescence. *Adv. Mater.* **2013**, *25*, 2440−2444.
(65) Orbach, R.; Wang, F.; Lioubashevsky, O.; Levine, R. D.; Remacle, F.; Willner, I. A Full-Adder Based on Reconfigurable DNA-Hairpin Inputs and DNAzyme Computing Modules. *Chem. Sci.* **2014**, *5*, 3381−3387.
(66) Kahan-Hanum, M.; Douek, Y.; Adar, R.; Shapiro, E. A Library of Programmable DNAzymes That Operate in a Cellular Environment. *Sci. Rep.* **2013**, *3*, 1535.
(67) Lund, K.; Manzo, A. J.; Dabby, N.; Michelotti, N.; Johnson-Buck, A.; Nangreave, J.; Taylor, S.; Pei, R.; Stojanovic, M. N.; Walter, N. G.; Winfree, E.; Yan, H. Molecular Robots Guided by Prescriptive Landscapes. *Nature* **2010**, *465*, 206−210.
(68) Tian, Y.; He, Y.; Chen, Y.; Yin, P.; Mao, C. A DNAzyme That Walks Processively and Autonomously Along a One-Dimensional Track. *Angew. Chem., Int. Ed.* **2005**, *44*, 4355−4358.
(69) Cha, T. G.; Pan, J.; Chen, H.; Salgado, J.; Li, X.; Mao, C.; Choi, J. H. A Synthetic DNA Motor That Transports Nanoparticles Along Carbon Nanotubes. *Nat. Nanotechnol.* **2014**, *9*, 39−43.
(70) Lin, H.; Zou, Y.; Huang, Y.; Chen, J.; Zhang, W. Y.; Zhuang, Z.; Jenkins, G.; Yang, C. J. DNAzyme Crosslinked Hydrogel: A New Platform for Visual Detection of Metal Ions. *Chem. Commun.* **2011**, *47*, 9312−9314.

DOI: 10.1021/acsami.5b02156
ACS Appl. Mater. Interfaces 2015, 7, 8923−8931